Synthesis and Characterization of Neutral Hexanuclear Iron Sulfur Clusters Containing Stair-like $[Fe_6(\mu_3\text{-}S)_4(\mu_2\text{-}SR)_4]$ and Nest-like $[Fe_6(\mu_3\text{-}S)_2(\mu_2\text{-}S)_2(\mu_4\text{-}S)(\mu_2\text{-}SR)_4]$ Core Structures†

Frank Osterloh,*,[1a] Wolfgang Saak,[1a] Siegfried Pohl,[1a,‡] Monika Kroeckel,[1b] Christian Meier,[1b] and Alfred X. Trautwein[1b]

Fachbereich Chemie, Carl von Ossietzky Universität Oldenburg, D-26111 Oldenburg, and Fachbereich Physik, Medizinische Universität Lübeck, D-23538 Lübeck, Germany

Received January 13, 1998

The binuclear iron complex $[\{Fe(\text{“}EtN_2S_2\text{”})\}_2]$ (**1b**, “EtN_2S_2” = *N*,*N*′-diethyl-3,7-diazanonane-1,9-dithiolate) was prepared from the free ligand and ferrous bis[bis(trimethylsilyl)amide] in toluene. In dichloromethane **1b** reacts with the $[Fe_4S_4I_4]^{2-}$ cubane cluster to displace two iodo ligands and to form the neutral hexanuclear cluster $[\{Fe(\text{“}EtN_2S_2\text{”})\}_2Fe_4S_4I_2]$ (**2**), which is isolated as black crystals in 87% yield. As elucidated by an X-ray structure analysis, **2** contains the novel hexanuclear stair-like $[Fe_6(\mu_3\text{-}S)_4(\mu_2\text{-}SR)_4]$ core, which exhibits crystallographic inversion symmetry. The compound crystallizes as a solvate with two molecules of CH_2Cl_2 per formula unit in the monoclinic space group $P2_1/n$ with $a = 1570.5(2)$ pm, $b = 1060.2(1)$ pm, $c = 1604.0(2)$ pm, $\beta = 114.93(1)°$, and $Z = 2$. In the aprotic polar solvents DMF, 1,2-propylenecarbonate, and DMSO, **2** dissolves with decomposition and formation of the cluster $[\{Fe(\text{“}EtN_2S_2\text{”})\}_2Fe_4S_5]$ (**3**), which is isolated as black needles from DMF. **3**·2DMF crystallizes in the triclinic space group $P\bar{1}$ with $a = 950.9(1)$ pm, $b = 1086.0(1)$ pm, $c = 2381.5(2)$ pm, $\alpha = 101.81(1)°$, $\beta = 91.94(1)°$, $\gamma = 97.01(1)°$, and $Z = 2$. The neutral compound contains a nest-like $[Fe_6(\mu_4\text{-}S)(\mu_3\text{-}S)_2(\mu_2\text{-}S)_2(\mu_2\text{-}SR)_4]$ core of idealized C_{2v} symmetry that is closely related to that of other well-known clusters, e.g., the cluster anion $[Fe_6S_9(SR)_2]^{4-}$. The zero-field ^{57}Fe Mössbauer spectrum of **3** is in accordance with four $Fe^{2.5+}S_4$ centers ($\delta = 0.46$ mm/s; $\Delta E_Q = 1.14$ mm/s) and two N_2S_3-bound high-spin Fe^{2+} sites ($\delta = 0.83$ mm/s; $\Delta E_Q = 3.64$ mm/s). A total cluster spin of 0 is deduced from the Mössbauer spectrum at 4.2 K and 5.3 T, which yields magnetic splitting from the applied field only. For **2**, three subspectra are observed in the Mössbauer spectrum (a, $\delta = 0.45$ mm/s, $\Delta E_Q = 1.05$ mm/s; b, $\delta = 0.55$ mm/s, $\Delta E_Q = 1.61$ mm/s, c, $\delta = 0.80$ mm/s; $\Delta E_Q = 3.83$ mm/s) reflecting different coordination environments of the iron atoms rather than different oxidation states. The electrochemical properties of **1b**, **2**, and **3** were determined by cyclic voltammetry. **1b** can be quasi-reversibly oxidized in dichloromethane solution at −75 mV (vs SCE). Whereas **2** shows only an irreversible redox behavior in *N*,*N*′-dimethylimidazolidin-2-one solution, **3** in the same solvent can be quasi-reversibly reduced in two consecutive steps at −830 and −1630 mV (vs SCE) to the dianion, which consists entirely of Fe(II).

Introduction

Iron sulfur clusters are present in many biological systems, where they participate in electron transfer reactions as well as in redox and nonredox catalysis.[2] Only recently has it been recognized that certain enzymes contain thiolate-bridged assemblies of the general formula $Fe_4S_4(\mu\text{-}X)M$, in which an Fe_4S_4 cubane is covalently linked to another metal ion by thiolate(s) or sulfide. In the case of Ni-containing CO-dehydrogenases/acetyl-CoA-synthases (CODH/ACS), M = Ni and X = SR or S,[3] whereas for sulfite reductase it has been proven that M = Fe and X = SR.[4] In an attempt to synthesize structural models for the thiolate-bridged assemblies in CODH/ACS, we recently investigated the reactivity of square planar Ni(II) complexes (Figure 1a) with the $[Fe_4S_4I_4]^{2-}$ anion.[5] As the metal-bound thiolate-S atoms in the Ni−aminothiolate complexes are still good nucleophiles, the Ni complexes are able to displace one or two iodo ligands from the $[Fe_4S_4I_4]^{2-}$ cluster to form anionic or neutral thiolate-bridged assemblies of an Fe_4S_4 cubane and one or two Ni(II) ions. As we will demonstrate here, the ability to form thiolate-bridged assemblies with an Fe_4S_4 cluster is not restricted to the Ni complexes. The iron complex **1b** (Figure 1b), of which derivatives have been

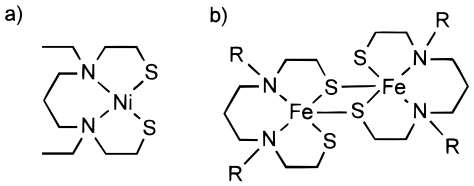

Figure 1. Schematic representations of (a) $[Ni(\text{“}EtN_2S_2\text{”})]$ and (b) $[\{Fe(\text{“}MeN_2S_2\text{”})\}_2]$ (R = CH_3, **1a**) and $[\{Fe(\text{“}EtN_2S_2\text{”})\}_2]$ (R = C_2H_5, **1b**).

* Corresponding E-mail adress: osterloh@sanctuary.harvard.edu.

† Dedicated to Professor Achim Müller on the occasion of his 60th birthday.

‡ Deceased.

(1) (a) Carl von Ossietzky Universität Oldenburg. (b) Medizinische Universität zu Lübeck.

(2) (a) *Iron-Sulfur Proteins*; Spiro, T. G., Ed.; Wiley-Interscience Publication: New York, 1982. (b) Holm, R. H.; Ciurli, S.; Weigel, J. A. *Prog. Inorg. Chem.* **1990**, *38*, 1 and literature cited therein. (c) Holm, R. H. *Adv. Inorg. Chem.* **1992**, *38*, 1 and literature cited therein.

(3) (a) Ragsdale, S. W.; Riordan, C. G. *JBIC* **1996**, *1*, 489. (b) Ragsdale, S. W.; Kumar, M. *Chem. Rev.* **1996**, *96*, 2515.

(4) Crane, B. R.; Siegel, L. M.; Getzoff, E. D. *Science* **1995**, *270*, 59.

(5) (a) Osterloh, F.; Saak, W.; Haase, D.; Pohl, S. *Chem. Commun*. **1996**, 777. (b) Osterloh, F.; Saak, W.; Pohl, S. *J. Am. Chem. Soc.* **1997**, *119*, 5648.

S0020-1669(98)00039-1 CCC: $15.00
Published on Web 06/24/1998

studied as early as 1972 by Lippard[6] and other groups,[7] reacts with $[Fe_4S_4I_4]^{2-}$ with displacement of two iodo ligands and formation of a neutral hexanuclear cluster with the novel stair-like $[Fe_6(\mu_3\text{-}S)_4(\mu_2\text{-}SR)_4]$ core. We report here on the crystal structure and other properties of this hexanuclear cluster and on its reaction with strong coordinating solvents yielding a cluster with a $[Fe_6(\mu_4\text{-}S)(\mu_3\text{-}S)_2(\mu_2\text{-}S)_2(\mu_2\text{-}SR)_4]$ core.

Experimental Section

Unless noted otherwise, all operations were carried out at room temperature under a pure dinitrogen atmosphere using gloveboxes and dried and degassed solvents. Methylene chloride was distilled from CaH_2, and dimethylformamide (DMF) was dried over P_4O_{10} for 72 h, distilled in vacuum, and degassed prior to use. Dimethyl sulfoxide (DMSO), 1,2-propylenecarbonate (PC), and 1,3-dimethylimidazolidin-2-one (DMI) were dried over molecular sieves (4 Å). Tetra(*n*-butylammonium)hexafluorophosphate (>99%) and ferric acetylacetonate were used as received. $(BTBA)_2[Fe_4S_4I_4]\cdot THF$ (BTBA = benzyltri(*n*-butyl)ammonium and *N*,*N*′-diethyl-3,7-diazanonane-1,9-dithiol ("EtN_2S_2"H_2) were synthesized as described earlier,[5b] and bis-[bis(trimethylsilyl)amido]iron(II) was synthesized according to Anderson et al.[8]

Bis[*N*,*N*′-diethyl-3,7-diazanonane-1,9-dithiolate-iron(II)] (1b). To a stirred solution of 0.560 g (2.23 mmol) of "N_2S_2"H_2 in 10 mL of toluene was added 1.00 g (2.23 mmol) of bis[bis(trimethylsilyl)amido]-iron(II). The solution immediately turned red, and an orange microcrystalline precipitate formed. The solution was stored overnight, and the solid was filtered off, washed with ether, and dried under reduced pressure. Yield: 0.58 g (0.96 mmol), 86%. IR (KBr): 2971m, 2957m, 2918s, 2841s, 1468s, 1451m, 1437m, 1379s, 1350, 1327w, 1302m, 1289w, 1277m, 1250w, 1209m, 1194m, 1181m, 1150w, 1119m, 1111m, 1098m, 1055m, 1040w, 1018s, 980m, 947m, 924w, 897w, 862w, 841w, 808w, 787w, 739s, 710s, 669m, 627w, 565w, 550w, 529w, 517m, 502w, 465w, 380w, 330s, 307s, 258m cm^{-1}. UV/vis (CH_2Cl_2): λ_{max} (ϵ) 525 (240), 440 (490), 360 (1460), 320 (3400), 300 (3400) nm (M^{-1} cm^{-1}). Anal. for $C_{11}H_{24}FeN_2S_2$: C, 43.42; H, 7.95; N, 9.21; S, 21.07 (calcd); C, 42.80; H, 7.90; N, 9.01; S, 20.89 (found). This compound can also be prepared in lower yields (16 %) from the ligand and ferric acetylacetonate in acetonitrile, using a 3-fold excess of the ligand for reduction of Fe(III).[6a]

$[\{Fe(\text{"}EtN_2S_2\text{"})\}_2Fe_4S_4I_2]\cdot 2CH_2Cl_2$ ($2\cdot 2CH_2Cl_2$). A solution of 1.35 g (0.909 mmol) of $(BTBA)_2[Fe_4S_4I_4]\cdot THF$ in 25 mL of CH_2Cl_2 was added to a solution of 0.554 g (0.910 mmol) of **1b** in 10 mL of the same solvent. On storing of the black solution for 24 h at room temperature, the product crystallized as black needles. This material was collected by filtration, washed with CH_2Cl_2, and dried under reduced pressure. Yield: 1.090 g (0.791 mmol), 87%. IR (KBr): 2967m, 2940m, 2922m, 2895m, 2859m, 1468s, 1437m, 1379s, 1350m, 1325w, 1306w, 1290m, 1275s, 1262s, 1223w, 1208m, 1179m, 1146m, 1113s, 1001s, 984s, 974s, 939w, 909w, 845w, 789m, 733s, 710s, 652m, 550s, 542s, 532m, 509w, 366s, 347s, 318s, 305m, 272m, 243m cm^{-1}. UV/vis (CH_2Cl_2): λ_{max} 590 (vw), 320 (s), 265 (vs) nm. Extinction coefficients were not determined due to the low solubility of the compound in CH_2Cl_2. Anal. for $C_{23}H_{50}Cl_2Fe_6I_2N_4S_8$: C, 21.27; H, 3.88; N, 4.31; S, 19.75 (calcd); C, 21.24; H, 4.08; N, 4.18; S, 19.10 (found).

$[\{Fe(\text{"}EtN_2S_2\text{"})\}_2Fe_4S_5\cdot 2$ DMF (3·2DMF). The preceding compound (0.200 g; 0.154 mmol) was dissolved in 20 mL of DMF with stirring. The black solution was filtered and then kept at room temperature for 24 h, during which time the product crystallized as black plates. These plates were collected by filtration, washed with DMF and subsequently with tetrahydrofuran, and dried under reduced pressure to afford 0.120 g (0.105 mmol), 68%. IR (KBr): 2953m, 2924m, 2884m, 2851m, 1670vs (DMF), 1466s, 1431s, 1402w, 1381s, 1352w, 1327w, 1308w, 1294m, 1277m, 1254m, 1225w, 1206m, 1179w, 1148w, 1113s, 1086s, 1055m, 1003s, 986s, 972m, 941w, 909w, 845w, 789w, 733s, 712s, 658s, 540m, 509w, 407vs, 363s, 339vs, 318s, 303w, 276m cm^{-1}. UV/vis (DMF): λ_{max} (ϵ) 530(vw), 335(s), 280(vs) nm. The solubility of the compound in CH_2Cl_2 was too low to determine extinction coefficients. Anal. for $C_{28}H_{62}Fe_6N_6O_2S_9$: C, 29.54; H, 5.49; N, 7.38; S, 25.34 (calcd); C, 29.59; H, 5.37; N, 7.35; S, 25.67 (found). **3** can also be obtained as a crystalline solid from DMSO or 1,2-propylenecarbonate by dissolving **2** in the minimum volume of the corresponding solvent and storing the black solution at room temperature. The identity of the three products has been determined by comparison of the IR spectra, which are virtually identical at wavenumbers around 350 cm^{-1}, i.e., in a range typical of Fe/S-core vibrations.[9]

Table 1. Crystal and Data Collection Parameters for $\mathbf{2}\cdot 2CH_2Cl_2$ and $\mathbf{3}\cdot$2DMF

compd	**2**	**3**
formula	$C_{24}H_{52}Cl_2Fe_6I_2N_4S_8$	$C_{28}H_{60}Fe_6N_6O_2S_9$
fw	1383.88	1136.46
temp (°C)	23(2)	23(2)
cryst syst	monoclinic	triclinic
space group	$P2_1/n$	$P\bar{1}$
A (pm)	1570.5(2)	950.9(1)
B (pm)	1060.2(1)	1086.0(1)
C (pm)	1604.0(2)	2381.5(2)
α (deg)		101.81(1)
β (deg)	114.93(1)	91.94(1)
γ (deg)		97.01(1)
V (pm^3)	$2421.9(5)\times 10^6$	$2359.8(4)\times 10^6$
Z	2	2
ρ_{calc} (g/cm^{-3})	1.898	1.599
λ (pm)	71.073	71.073
μ (cm^{-1})	36.13	22.26
cryst dimens (mm)	$0.45\times 0.38\times 0.11$	$0.36\times 0.16\times 0.10$
data collected	3785	6555
unique data	3785	6555
data [$I > 2\sigma(I)$]	2598	4009
R1[a] [$I > 2\sigma(I)$]	0.0492	0.0566
wR2[b] [$I > 2\sigma(I)$]	0.1036	0.1122

[a] $R1 = \sum||F_o| - |F_c||/\sum|F_o|$. [b] $wR2 = \{\sum[w(F_o^2 - F_c^2)^2]/\sum[w(F_o^2)^2]\}^{1/2}$.

X-ray Structure Determinations. Crystal and data collection parameters of **2** and **3** are summarized in Table 1 together with refinement parameters. Single crystals of the compounds were obtained as described in the preparative section.

$[\{Fe(\text{"}EtN_2S_2\text{"})\}_2Fe_4S_4I_2]$ (**2**) crystallizes as a solvate with two molecules of dichloromethane per formula. A black single crystal of $\mathbf{2}\cdot 2CH_2Cl_2$ was sealed in a glass capillary and mounted on a Siemens-Stoe AED 2 four-circle diffractometer. Data collection using Mo Kα radiation and $\omega-2\theta$ scans gave 3785 independent reflections (θ_{max} = 24°), of which 2598 with $I > 2\sigma(I)$ were used in all calculations. No absorption correction was applied. The structure was solved by direct methods and the solution developed using full-matrix least-squares refinement on F^2 and difference Fourier synthesis.[10] Anisotropic displacement parameters were refined for all non-H atoms, except those of the solvent molecule, which was refined with idealized geometry on three positions with occupancy factors of 0.5, 0.25, and 0.25, respectively. H atoms were included on calculated positions with isotropic displacement parameters tied to those of the corresponding carbon atoms. At convergence, R1 = 0.0492, wR2 = 0.1036, and GOF = 1.020 for 226 parameters.

A black prism-shaped crystal (0.36 × 0.16 × 0.10 mm) of $[\{Fe(\text{"}EtN_2S_2\text{"})\}_2Fe_4S_5]\cdot$2DMF (**3**·2DMF) was sealed in a glass capillary. Data collection which was performed according to the above described procedures gave 6555 independent reflections (θ_{max} = 23°), of which 4009 with $I > 2\sigma(I)$ were used in all calculations. No absorption correction was applied. The structure was solved by direct methods,

(6) (a) Karlin, K. D.; Lippard, S. J. *J. Am. Chem. Soc.* **1976**, *98*, 6951. (b) Hu, W.-J.; Lippard, S. J. *J. Am. Chem. Soc.* **1974**, *96*, 2366.
(7) Mills, D. K.; Hsiao, Y. M.; Farmer, P. J.; Atnip, E. V.; Reibenspies, J. H.; Darensbourg, M. Y. *J. Am. Chem. Soc.* **1991**, *113*, 1421.
(8) Andersen, R. A.; Faegri, K., Jr.; Green; J. C.; Haaland, A.; Lappert, M. F.; Leung, W.-P.; Rypdal, K. *Inorg. Chem.* **1988**, *27*, 1782.
(9) Nakamoto, K. *Infrared and Raman Spectra of Inorganic and Coordination Compounds*, 4th ed.; Wiley: New York, 1986; 436 pp.
(10) Sheldrick, G. M., Göttingen, Germany, 1990, 1993.

Scheme 1. Synthesis of **1b** in Toluene and Reaction with $[Fe_4S_4I_4]^{2-}$ in Dichloromethane Leading to **2**. Formation of **3** from **2**

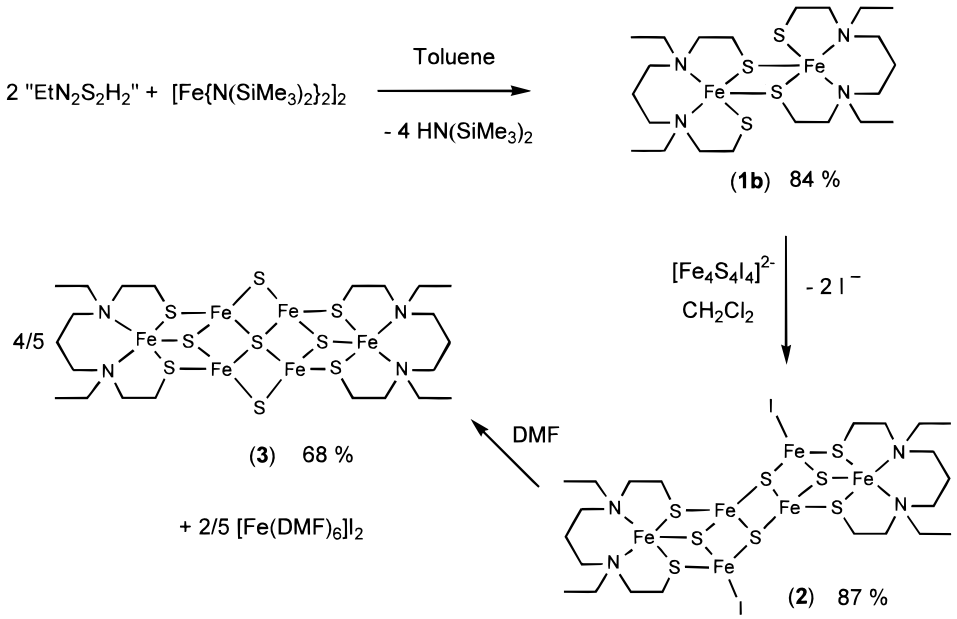

and full-matrix least-squares refinement was on F^2.[10] Anisotropic displacement parameters were refined for all non-H atoms, and H atoms were treated as described for **2**. At convergence, R1 = 0.0566, wR2 = 0.1122, and GOF = 1020 for 402 parameters.

Other Physical Measurements. Strictly anaerobic conditions were employed for all measurements. IR spectra were recorded with a Biorad FTS-7 spectrometer using KBr pellets. Electronic absorption spectra were obtained on a Shimadzu UV-260 spectrophotometer by using 0.1 mm path length quartz cells. Cyclic voltammograms were recorded using a three-electrode cell employed with two Pt electrodes and a SCE and with a 0.1 M (n-Bu_4N)PF_6 solution as supporting electrolyte. ^{57}Fe Mössbauer spectra were recorded with a conventional constant-acceleration spectrometer using a 1.85 GBq ^{57}Co source in a Rh matrix. Measurements at 4.2 K were performed using a bath cryostat (VariOx 306-Oxford Instruments) with a permanent magnet mounted outside the cryostat producing a field of 10 mT. High-field measurements (5.35 T) were performed with a cryostat equipped with a superconducting magnet (Oxford Instruments). The spectra were analyzed assuming Lorentzian line shape, and the isomer shift is quoted relative to α-Fe at room temperature.

Results and Discussion

Diiron complexes like **1a** (Figure 1a) of chelating ligands with a 3,7-diazanonane-1,9-dithiol backbone have been well investigated.[6,7] They contain two Fe(II) ions in trigonal-bipyramidal or square-pyramidal coordination environments and form thiolate-bridged dimers as a result of the nucleophilicity of the thiolate-S atoms and because of the tendency of Fe(II) to achieve a coordination sphere of five atoms in this mixed sulfur−nitrogen environment. We prepared the complex **1b** by metathesis from ferrous bis[bis(trimethylsilyl)amide][8] and *N*,*N*′-diethyl-3,7-diazanonane-1,9-dithiol in toluene (Scheme 1). This method is an improvement of the former syntheses using the dithiol and ferric acetylacetonate or the disulfide of the ligand and iron pentacarbonyl, respectively,[6] since it gives the complex as an orange microcrystalline powder in an increased yield of 84%, based on the free ligand. Like **1a**, the complex **1b** is very soluble in dichloromethane and slightly soluble in DMF, acetonitrile, or toluene. The similar solubility suggests that **1b** is also a dimer.

When solutions containing **1b** and the $[Fe_4S_4I_4]^{2-}$ anion as its benzyltri-*n*-butylammonium salt are combined in dichloromethane at room temperature, an immediate color change to deep black is observed. Upon storage of the solution at room temperature for 24 h, the cluster **2** separates as black needles, which were isolated in 87% yield (Scheme 1). Spectroscopic and analytical data of the black crystals are in accordance with a neutral hexanuclear cluster that has formed by displacement of two iodo ligands of the $[Fe_4S_4I_4]^{2-}$-cluster anion by the diiron complex **1b**. X-ray crystallography revealed that **2** no longer contains an Fe_4S_4 cubane but instead adopts the previously unobserved stair-like $[Fe_6(\mu_3\text{-}S)_4(\mu_2\text{-}SR)_4]$ core, which is presented in Figure 2. We believe that only two steps are involved in the formation of **2**, i.e., the substitution of two iodo ligands on $[Fe_4S_4I_4]^{2-}$ by thiolate from **1b** followed by a rearrangement reaction, which is depicted in Scheme 2. This rearrangement involves (a) the breakage of two opposite Fe−S bonds of the Fe_4S_4 cube induced by an interaction of the coordinatively unsaturated N_2S_2-bound Fe(II) ions with two sulfides of the Fe_4S_4 cubane cluster and (b) the unfolding of the Fe_4S_4 cube to give the stair-like Fe_4S_4 fragment in **2**. This cluster interconversion reaction demonstrates the effect of a Lewis acid in the vicinity of an Fe_4S_4 core, which must be regarded as a key step in the formation of clusters of higher nuclearity from Fe_4S_4 cubane clusters. The reaction further raises the question, if similar rearrangements might occur in Ni-containing CO-dehydrogenases/acetyl-CoA-synthases (CODH/ACS), where a single nickel center interacts with an Fe_4S_4 cubane cluster.[3,5] Without degradation the novel cluster **2** is soluble in 1,3-

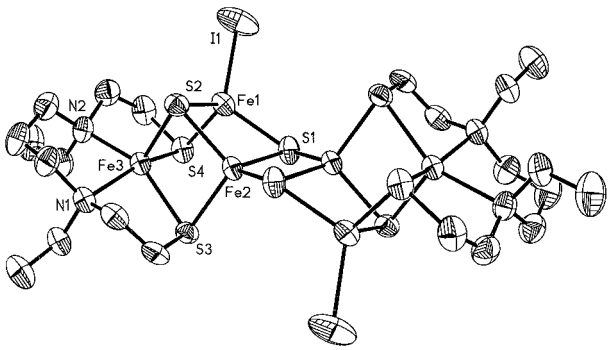

Figure 2. X-ray crystal structure of **2** with atom-labeling scheme. Thermal ellipsoids are shown at the 50% probability level; H atoms are omitted. The molecule exhibits crystallographic inversion symmetry.

Scheme 2. Simplified Mechanism of the Formation of the Hexanuclear Cluster **2** from the Fe_4S_4 Cubane and the Binuclear Complex **1b**[a]

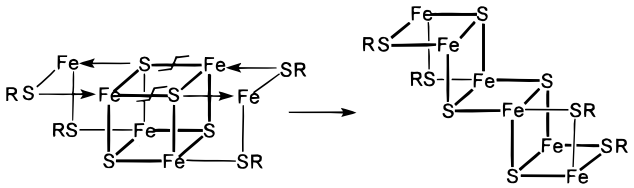

[a] In a hypothetical transition state the two Fe atoms and two S atoms of **1b** bind to two opposite Fe and S atoms of the Fe_4S_4 cluster. This interaction induces the cleavage of two Fe−S bonds of the Fe_4S_4 cube and initiates the rearrangement to a stair-like structure.

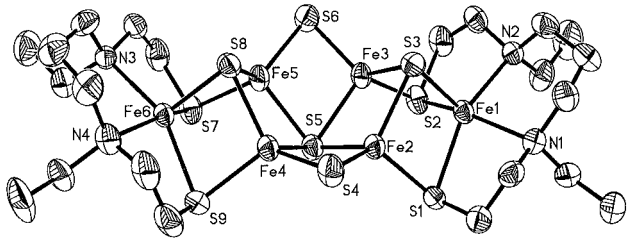

Figure 3. Crystallographic structure of **3** with atom-labeling scheme. Thermal ellipsoids are shown at the 50% probability level; H atoms are omitted.

dimethylimidazolidine-2-one and slightly soluble in dichloromethane. In polar aprotic solvents, e.g., DMF, DMSO, or 1,2-propylenecarbonate, **2** dissolves rapidly, generating black solutions, from which the cluster **3** separates as a crystalline black solid (Scheme 1). In the case of DMF as a solvent the crystals were sufficient for X-ray crystallography. The structure analysis showed that a novel hexanuclear cluster with a $[Fe_6(\mu_4\text{-S})(\mu_3\text{-S})_2(\mu_2\text{-S})_2(\mu_2\text{-SR})_4]$ core had formed from **2**, formally by substitution of two iodo ligands in **2** by 1 equiv of sulfide. The sulfide is liberated from **2**, which decomposes in DMF as a consequence of the lability of Fe−I bonds toward strong coordinating solvents.[11] Accordingly, from 5 equiv of the starting material are formed 4 equiv of **3** with an actual yield of 68%, based on this stoichiometry. $[Fe(DMF)_6]I_2$ has been isolated as a byproduct of this reaction and identified by means of IR spectroscopy.

Description of the Structures

2 (Figure 2) crystallizes with two molecules of dichloromethane and **3** (Figure 3) with two molecules of DMF. Both compounds form isolated neutral species in the solid state with no unusual close contacts to the solvents. Selected interatomic distances and angles are collected in Table 2.

The neutral hexanuclear cluster **2** exhibits crystallographic inversion symmetry and contains Fe atoms in square-pyramidal N_2S_3 (Fe(3)), tetrahedral S_4 (Fe(2)), and S_3I environments (Fe(1)). The μ_3-sulfide- and μ_2-thiolate-bridged Fe centers (two Fe(III) and 4 Fe(II)) are located in seven prism-like Fe_2S_2 fragments that share common edges. Of these, five prisms (excluding those in which S(3) and S(3′) are involved) are arranged in a stair-like shape, i.e., these prisms form a line in which the least-squares planes of the Fe_2S_2 prisms are arranged vertically and horizontally in an alternating manner. Despite the folding, which is a result of the binding properties of the S atoms and of the geometry of the tetracoordinate Fe centers, all Fe atoms of the stair-like $[Fe_6(\mu_3\text{-S})_4(\mu_2\text{-SR})_4]$ core roughly form one common plane with an average deviation of only 6.9 pm.

The Fe(1)−Fe(2) distance of 260.6(2) pm not only is considerably shorter than the remaining Fe−Fe distances within the cluster (average value of all distances 277.3 pm) but to our knowledge is the shortest Fe−Fe distance observed in a Fe/S cluster with σ-donor ligands only. Similar Fe−Fe distances were found in $[Fe_4S_3(NO)_4(PPh_3)_3]$ (257.1−278.0 pm)[15b] and in $[Fe_4S_4(C_5H_5)_4]$ (261.8−265.0 pm).[12] The other structural parameters of **2** are typical. The Fe(2)−Fe(2′) distance of 270.3(2) pm is only slighty shorter than in symmetrically substituted $[Fe_4S_4X_4]^{2-}$ cubanes (X = Hal^-, RS^-) (Fe−Fe: 273.0 to 277.6 pm),[13] and expectedly, the Fe−Fe and Fe−S distances, which appear with the pentacoordinate Fe atoms, are longer than those between four-coordinate Fe atoms.

The coordination environments of the pentacoordinated Fe atoms differ significantly in **2** and in **1a**. Whereas the N_2S_3-bound Fe(3) in **1a** was in a trigonal-bipyramidal coordination environment, in **2** it is bound square-pyramidally by four donor atoms of the chelating ligands and one axial sulfide of the central $Fe_4S_4I_2$ unit. The metal ion is located 51 pm above the least-squares plane of the basal atoms. Interestingly, the change of coordination is accompanied by a decrease of the average Fe−S distance (240.9 pm in **1a**, 237.7 pm in **2**) but not of the Fe−N distances. This might be interpreted in terms of significant strain in $[\{Fe(\text{“}MeN_2S_2\text{”})\}_2]$ (**1a**) and in a slightly more oxidized character of this Fe ion in **2**. Cluster **2** is significantly different from other known hexanuclear clusters, i.e., those with basket-[14] and prism-like,[15] octahedral,[16] and nest-like structures (like the $[Fe_6S_9(SR)_2]^{4-}$ anion).[17] However, it displays some similarity to the dicubane cluster $[\{Fe_4S_4(PR_3)_3\}_2]$,[18] whose Fe/S core can easily be derived from that of **2** by capping the cuboidal Fe_3S_4 fragments with two additional Fe atoms.

Cluster **3** possesses idealized C_{2v} symmetry in the solid state. As in **2** all six tetrahedrally or pyramidally coordinated Fe atoms (two Fe(III) and four Fe(II)) are located in one common plane but with a smaller standard deviation of 2.8 pm. The cluster contains sulfur in four different bridging modes, i.e., μ_2-, μ_3-, and μ_4-sulfide and μ_3-thiolate S atoms. The expected increase in the average Fe−S bond lengths is pronounced for the Fe−μ_2-S (219.9 pm) and Fe−μ_3-S distances (230.2 pm), but not for the Fe−μ_4-S distances (231.2 pm), which are equal to the bond lengths between μ_3-thiolate S and the four-coordinate Fe

(11) Similar degradation reactions have been observed with $[Fe_4S_4I_4]^{2-}$ in DMF or DMSO.

(12) (a) Schunn, R. A.; Fritchie, C. J., Jr.; Prewitt, C. T. *Inorg. Chem.* **1966**, *5*, 892. (b) Wei, C. H.; Wilkes, G. R.; Treichel, P. M.; Dahl, L. D. *Inorg. Chem.* **1966**, *5*, 900.

(13) (a) Pohl, S; Saak, W. *Z. Naturforsch.* **1988**, *43b*, 457 and literature cited therein. (b) Mascharak, P. K.; Hagen, K. S.; Spence, J. T.; Holm, R. H. *Inorg. Chim. Acta* **1983**, *80*, 157.

(14) (a) Snyder, B. S.; Holm, R. H. *Inorg. Chem.* **1990**, *29*, 274. (b) Snyder, B. S.; Holm, R. H. *Inorg. Chem.* **1988**, *27*, 2339. (c) Chen, C.; Cai, J.; Liu, Q.; Wu, D.; Lei, X.; Zhao, K.; Kang, B.; Lu, J. *Inorg. Chem.* **1990**, *29*, 4878. (d) Harmjanz, M.; Junghans, C.; Opitz, U.-A.; Bahlmann, B.; Pohl, S. *Z. Naturforsch.* **1996**, *51b*, 1040.

(15) (a) Saak, W.; Henkel, G.; Pohl, S. *Angew. Chem., Int. Ed. Engl.* **1984**, *23*, 153. (b) Scott, M. J.; Holm, R. H. *Angew. Chem., Int. Ed. Engl.* **1993**, *32*, 564. (c) Kanatzidis, M. G.; Hagen, W. R.; Dunham, W. R.; Lester, R. K.; Coucouvanis, D. *J. Am. Chem. Soc.* **1985**, *107*, 953.

(16) (a) Cecconi, F.; Ghilardi, C. A.; Midollini, S.; Orlandini, A.; Zanello, P. *J. Chem. Soc., Dalton Trans.* **1987**, 831. (b) Cecconi, F.; Ghilardi, C. A.; Midollini, S. *J. Chem. Soc., Chem. Commun.* **1981**, 640.

(17) (a) Christou, G.; Holm, R. H.; Sabat, M.; Ibers, J. A. *J. Am. Chem. Soc.* **1981**, *103*, 6269. (b) Christou, G.; Sabat, M.; Ibers, J. A.; Holm, R. H. *Inorg. Chem.* **1982**, *21*, 3518. (c) Hagen, K. S.; Watson, A. D.; Holm, R. H. *J. Am. Chem. Soc.* **1983**, *105*, 3905. (d) Strasdeit, H.; Krebs, B.; Henkel, G. *Inorg. Chem.* **1984**, *23*, 1816.

(18) (a) Cai, L.; Segal, B. M.; Long, J. R.; Scott, M. J.; Holm, R. H. *J. Am. Chem. Soc.* **1995**, *117*, 8863. (b) Goh, C.; Segal, B. M.; Huang, J.; Long, J. R.; Holm, R. H. *J. Am. Chem. Soc.* **1996,** *118*, 11844.

Table 2. Selected Interatomic Distances (pm) and Angles (deg) for **2** and **3**

2		**3**			
Fe(1)−Fe(2)	260.6(2)	Fe(1)−Fe(2)	285.9(2)	Fe(2)−Fe(3)	264.3(2)
Fe(1)−Fe(3)	293.7(2)	Fe(1)−Fe(3)	290.1(2)	Fe(4)−Fe(5)	267.6(2)
Fe(2)−Fe(3)	284.7(2)	Fe(4)−Fe(6)	287.4(2)	Fe(2)−Fe(4)	271.1(2)
Fe(2)−Fe(2′)[a]	270.3(2)	Fe(5)−Fe(6)	290.4(2)	Fe(3)−Fe(5)	272.9(2)
mean:	277.3			mean: 278.7	
Fe(1)−S(1)	229.8(2)	Fe(2)−S(4)	219.6(3)	Fe(2)−S(3)	230.2(3)
Fe(1)−S(2)	230.4(2)	Fe(3)−S(6)	219.5(3)	Fe(3)−S(3)	231.3(3)
Fe(1)−S(4)	231.3(2)	Fe(4)−S(4)	220.3(3)	Fe(4)−S(8)	229.3(3)
Fe(1)−I(1)	256.2(2)	Fe(5)−S(6)	220.3(3)	Fe(5)−S(8)	229.9(2)
		mean:	219.9	mean:	230.2
Fe(2)−S(1)	228.8(2)	Fe(2)−S(5)	230.8(3)	Fe(4)−S(9)	231.9(3)
Fe(2)−S(2)	229.2(2)	Fe(3)−S(5)	232.2(3)	Fe(5)−S(7)	233.2(3)
Fe(2)−S(3)	229.8(2)	Fe(4)−S(5)	230.5(3)	Fe(3)−S(2)	231.6(2)
Fe(2)−S(1′)	222.3(2)	Fe(5)−S(5)	231.4(3)	Fe(2)−S(1)	230.4(3)
		mean:	231.2	mean:	231.8
Fe(3)−N(1)	224.8(6)	Fe(1)−N(1)	224.1(7)	Fe(6)−N(3)	222.2(7)
Fe(3)−N(2)	222.0(6)	Fe(1)−N(2)	227.3(7)	Fe(6)−N(4)	226.0(6)
Fe(3)−S(2)	231.9(2)	Fe(1)−S(1)	240.2(3)	Fe(6)−S(7)	243.8(3)
Fe(3)−S(3)	238.9(2)	Fe(1)−S(2)	241.3(3)	Fe(6)−S(8)	228.6(2)
Fe(3)−S(4)	242.4(2)	Fe(1)−S(3)	229.0(2)	Fe(6)−S(9)	240.4(3)
N(1)−Fe(3)−N(2)	90.8(2)	N(1)−Fe(1)−N(2)	89.6(2)	N(3)−Fe(6)−N(4)	90.6(3)
N(1)−Fe(6)−S(2)	102.9(2)	N(1)−Fe(1)−S(1)	81.6(2)	N(3)−Fe(6)−S(7)	82.2(2)
N(1)−Fe(3)−S(3)	81.4(2)	N(1)−Fe(1)−S(2)	153.5(2)	N(3)−Fe(6)−S(8)	104.4(2)
N(1)−Fe(3)−S(4)	157.5(2)	N(1)−Fe(1)−S(3)	106.5(2)	N(3)−Fe(6)−S(9)	154.5(2)
N(2)−Fe(3)−S(2)	108.0(2)	N(2)−Fe(1)−S(1)	154.4(2)	N(4)−Fe(6)−S(7)	156.8(2)
N(2)−Fe(3)−S(3)	151.8(2)	N(2)−Fe(1)−S(2)	81.2(2)	N(4)−Fe(6)−S(8)	102.6(2)
N(2)−Fe(3)−S(4)	82.3(2)	N(2)−Fe(1)−S(3)	103.9(2)	N(4)−Fe(6)−S(9)	82.0(2)
S(2)−Fe(3)−S(3)	100.21(8)	S(1)−Fe(1)−S(2)	96.08(9)	S(7)−Fe(6)−S(8)	100.6(1)
S(2)−Fe(3)−S(4)	99.65(8)	S(1)−Fe(1)−S(3)	101.62(9)	S(7)−Fe(6)−S(9)	95.0(1)
S(3)−Fe(3)−S(4)	94.55(8)	S(2)−Fe(1)−S(3)	99.91(9)	S(8)−Fe(6)−S(9)	101.1(1)

[a] Symmetry operation for the equivalent atoms: $-x + 1, -y, z + 2$.

atoms (231.8 pm). The Fe−Fe distances in **3** can be grouped in three sets. The shortest occur in the central Fe_4S_5 unit of the molecule. Those distances which parallel the longer molecular axis of **3** are longer (271.1(2)−272.9(2) pm) than those which are perpendicular to this axis (264.3(2)−267.6(2) pm). The Fe−Fe distances between the four- and five-coordinate Fe atoms (285.9(2)−290.4(2) pm) are very long, which is clearly a result of the higher coordination number of the latter. The nest-like $[Fe_6S_9]$ core of **3** is closely related to that of other clusters with equal or higher nuclearity. Whereas the central Fe_4S_5 fragment of **3** is contained in the basket clusters $[Fe_6S_6X_2(PR_3)_4]$[14] (X = Hal$^-$, RS$^-$) and in members of the $[Fe_8S_6I_8]^{n-}$ cluster family,[19] the whole Fe_6S_9 unit is found in $[Na_2Fe_{18}S_{30}]^{8-}$,[20] in the $[Fe_6S_9(SR)_2]^{4-}$ anions (R = Bu^t,[17a−c] Ph,[17a−c] Et,[17d] CH_2Ph,[17d]) and in $[Na_2\{Fe_6S_9(SR)_2\}]^{6-}$.[17d]

The structure of the $[Fe_6S_9(SR)_2]^{4-}$ cluster is depicted in Figure 4. When compared to **3**, the terminal thiolate bound Fe atoms in the tetraanion exhibit shorter distances to the adjacent Fe atoms (268.5 pm on average compared to 288.5 pm in **3**), which is clearly a result of the lower coordination number of the former. However, despite the different nature of bridging μ_3-S atoms (μ_3-SR in **3**, μ_3-S in the dianion), the central Fe_4S_5 units in both compounds are congruent. This is surprising since the average Fe oxidation state of +2.33 in **3** is lower than in $[Fe_6S_9(SR)_2]^{4-}$, where it is +2.67. However, if one assumes that the additional two electrons in **3** are predominantly located on the N_2S_3-bound Fe centers, the mean oxidation state of the Fe ions incorporated in the central Fe_4S_5 units with +2.5 and +2.67 are almost equal. Indeed, this charge distribution is confirmed by the results of ^{57}Fe Mössbauer spectroscopy (vide infra).

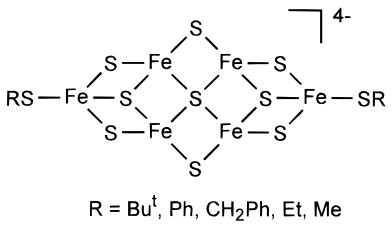

Figure 4. Structure of the related $[Fe_6S_9(SR)_2]^{4-}$ cluster anion.

^{57}Fe Mössbauer Spectra

^{57}Fe Mössbauer spectra of **3** and **2** obtained at 4.2 K in low (10 mT) and high (5.35 T) fields are shown in Figures 5 and 6. The low-field spectrum of **3** shows two quadrupole doublets with intensity ratio 1:2 (Figure 5a, Table 3). The less intense signal (1) with the larger quadrupole splitting is assigned to the two N_2S_3-bound Fe centers whereas the other signal (2) is assigned to the four indistinguishable tetrahedral FeS_4 sites. Comparing isomer shift and quadrupole splitting of subspectrum 1 with those of the dimeric complex **1a**, which contains two ferrous high-spin iron sites, suggests that also the FeS_3N_2 centers in **3** contain ferrous high-spin iron. The isomer shift of (subspectrum 2) is intermediate between the values typical for $Fe^{2+}S_4$ ($\delta \approx 0.65$ mm/s) and $Fe^{3+}S_4$ ($\delta \approx 0.25$ mm/s), suggesting a formal oxidation state of 2.5+ for the four FeS_4 sites.[21] The low-field spectra of **2** have been fitted with three quadrupole doublets of equal intensity. There are several combinations of isomer shifts and quadrupole splittings which

(19) (a) Pohl, S.; Saak, W. *Angew. Chem., Int. Ed. Engl.* **1984**, *23*, 907. (b) Saak, W.; Pohl, S. *Angew. Chem., Int. Ed. Engl.* **1991**, *30*, 881. (c) Pohl, S.; Opitz, U. *Angew. Chem., Int. Ed. Engl.* **1993**, *32*, 863.
(20) (a) You, J.-F.; Snyder, B. S.; Papaefthymiou, G. C.; Holm, R. H. *J. Am. Chem. Soc.* **1990**, *112*, 1067. (b) You, J.-F.; Snyder, B. S.; Holm, R. H. *J. Am. Chem. Soc.* **1988**, *110*, 6589.

Table 3. Isomer Shifts δ, Quadrupole Splittings ΔE_Q, and Asymmetry Parameters η of **1a**, **2**, and **3**

compd	site	δ^a (mm/s)	ΔE_Q (mm/s)	coordination	η	no. of iron sites
[{Fe("MeN_2S_2")}$_2$] (**1a**)[b]	1	0.88	3.45	FeS_3N_2		1
[{Fe("EtN_2S_2")}$_2Fe_4S_4I_2$] (**2**)	1	0.45	1.05	FeS_4	0.9	2
	2	0.55	1.61	FeS_3I	0.7	2
	3	0.80	3.83	FeS_3N_2	0.1	2
[{Fe("EtN_2S_2")}$_2Fe_4S_5$] (**3**)	1	0.83	3.64	FeS_3N_2	0.1	2
	2	0.46	1.14	FeS_4	0.9	4

[a] Versus α-Fe at room temperature. [b] From Karlin and Lippard.[6a]

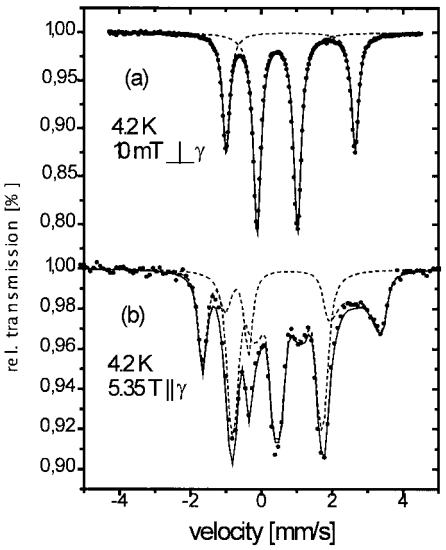

Figure 5. ^{57}Fe Mössbauer spectra of [{Fe("EtN_2S_2")}$_2Fe_4S_5$] (**3**) measured at 4.2 K in fields of (a) 10 mT ⊥ γ and (b) 5.35 T || γ.

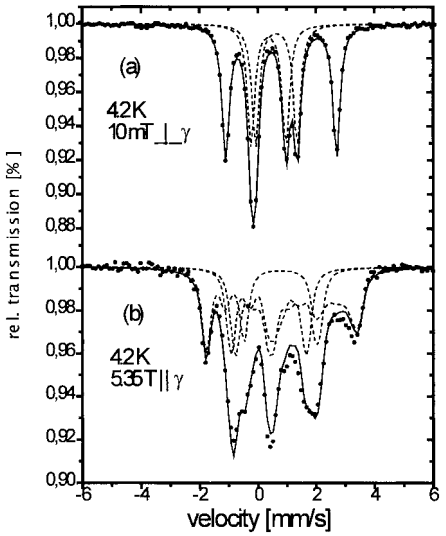

Figure 6. ^{57}Fe Mössbauer spectra of [{Fe("EtN_2S_2")}$_2Fe_4S_4I_2$] (**2**) measured at 4.2 K in fields of (a) 10 mT ⊥ γ and (b) 5.35 T || γ.

fit the spectra, but only one of them is physically meaningful. These parameters are summarized in Table 3. Two subspectra, 1 and 3, have parameters very similar to those of **3**. Hence, they are assigned according to the sites described above for **3**, while subspectrum 2 is assigned to FeS_3I centers. The slightly larger isomer shift of subspectrum 2 compared to FeS_4 is probably only a result of the subsitution of sulfur by iodine. In conclusion, **2** exhibits properties similar to those of **3**, i.e., the

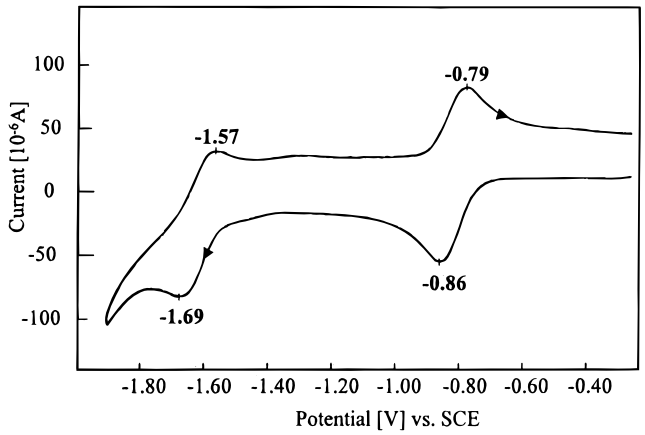

Figure 7. Cyclic voltammogram of a 0.70×10^{-3} M solution of **3** in 1,3-dimethylimidazolidin-2-one. The scan rate was 200 mV/s. Peak potentials (V) were referenced against SCE.

Table 4. Electrochemical Data for **1b**, **2**, and **3**

	solvent	$E_{1/2}$ (mV)	ΔE_p (mV)	I_{p_a}/I_{p_c}[a]	scan rate (mV/s)
1b	CH_2Cl_2	−75	90	0.51	100
2	DMI	+490			
		−810			
3	DMI	−830	70	0.92	200
		−1630	120	0.63	

[a] Ratio of peak currents, corrected according to ref 22.

two terminal FeS_3N_2 centers represent ferrous high-spin sites (Fe^{2+}), and the central FeS_4 or FeS_3I moieties represent fully delocalized mixed-valence ($Fe^{2.5+}$) sites. Furthermore, both six-Fe clusters exhibit similar spin coupling with cluster spin $S_{tot} = 0$, as seen in the spectra obtained at 4.2 K in large fields (Figures 5b and 6b). These spectra have been simulated assuming zero Fermi-contact contribution.

Electrochemical Studies

A cyclic voltammogram of **3** is shown in Figure 7, and electrochemical data of **1b**, **2**, and **3** are summarized in Table 4. All potentials are referenced against the saturated calomel electrode. **2** can be irreversibly oxidized at +490 mV in dichloromethane solution. This potential is slightly higher for **2** than for the negatively charged parent cluster $[Fe_4S_4I_4]^{2-}$ (+435 mV; $I_a/I_c = 1$ in CH_2Cl_2), which can be explained by the overall neutral charge of **2**. The reduction at −810 mV is again irreversible. This is probably a result of the presence of the iodo ligands, which cannot stabilize low oxidation states of iron. In contrast, **3** is quasi-reversibly reduced to the dianion in two consecutive steps at −830 and −1630 mV. The resultant totally reduced $[Fe_6(\mu\text{-}S)_5(\mu\text{-}SR)_4]^{2-}$ core of $[(\mathbf{3})]^{2-}$ contains iron entirely in the ferrous oxidation state and can be viewed as the counterpart of the $[Fe_6S_9(SBu^t)_2]^{3-}$, ion which presumably has the same structure but is much more oxidized. The latter cluster anion contains five Fe(III) and one Fe(II) and has been

(21) (a) Trautwein, A. X.; Bill, E.; Bominaar, E. L.; Winkler, H. *Struct. Bonding* **1991**, *78*, 1. (b) Schulz, C.; Debrunner, P. G. *J. Phys., Colloq.* **1976**, C6−153.
(22) Nicholson, R. S. *Anal. Chem.* **1966**, *38*, 1406.

observed in DMSO solution as a one electron oxidation product ($E_{1/2} = -0.62$ V vs SCE) from the corresponding tetraanion.[17a]

Summary

The reaction of the thiolate-bridged diiron complex **1b** with the $[Fe_4S_4I_4]^{2-}$ ion leads to a novel hexanuclear cluster **2** which complements the row of known hexanuclear clusters, i.e., those with basket-[14] and prism-like,[15] octahedral,[16] and nest-like structures (like the $[Fe_6S_9(SR)_2]^{4-}$ anion).[17] In aprotic polar solvents **2** decomposes, forming the neutral hexanuclear cluster **3**, which contains a nest-like $Fe_6S_5(SR)_4$ core similar to that of the known $[Fe_6S_9(SR)_2]^{4-}$ anion. Both compounds **2** and **3** exhibit spin coupling of two ferrous high-spin sites with four mixed-valent sites yielding a total cluster spin of $S_{tot} = 0$. Whereas **2** exhibits only irreversible redox behavior, **3** can be consecutively reduced to the dianion, which consists entirely of Fe(II).

Acknowledgment. This research was supported by the Deutsche Forschungsgemeinschaft and the BMBF. We thank Dr. C. Walsdorff and B. Segal for helpful comments on the manuscript.

Supporting Information Available: Complete list of atomic coordinates and anisotropic atomic displacement parameters of all non-hydrogen atoms (5 pages). Ordering information is given on any current masthead page.

IC980039T